Research Article

Wojciech Jankowski* and Juliusz Sołkowski

The modelling of railway subgrade strengthening foundation on weak soils

https://doi.org/10.1515/eng-2022-0053
received July 05, 2021; accepted June 14, 2022

Abstract: As a consequence of increased axle loads and speeds of trains on modernised railway lines, there may occur problems with bearing capacity and stability of the subgrade in some sections of the railway network. This is the situation we are dealing with right now on the Polish State Railways network. Therefore, as a case study, a fragment of an existing railway embankment based on a weak foundation was chosen for the analysis of train–track–subgrade interaction. A two-stage train–track–subgrade model has been developed. The model consists of the upper part (train–track) and the lower part (subgrade-foundation). The first part is modelled as a self-contained system of differential equations which are solved by means of finite difference method and yield the stress levels on the subgrade. These stresses are treated as a load for the lower system modelled using FEM. The model has been validated using experimental data from literature, authors' measurements, and railway staff measurements of the track geometry. Several cases of strengthening methods were calculated and compared with measurements on the railway section under consideration. Good agreement between the prediction and the measurement was found. The novelty of the model is including the heterogeneity of the subgrade, the strengthening methods, and very deep layers of its foundation as well as adding the influence of vibration on the weakening of soils. It was found that this influence is noticeable and should be included in the prediction of railway subgrade behaviour

Keywords: ballasted railway track, subgrade strengthening, weak soils

*** Corresponding author: Wojciech Jankowski,** Civil Engineering Department, Cracow University of Technology, 24 Warszawska St., 31-155 Cracow, Kraków, Poland,
e-mail: wojciech.jankowski@pk.edu.pl
Juliusz Sołkowski: Civil Engineering Department, Cracow University of Technology, 24 Warszawska St., 31-155 Cracow, Kraków, Poland, e-mail: jsolkow@pk.edu.pl

1 Introduction

As a consequence of increased axle loads and speeds of trains on modernised railway lines, problems may occur with bearing capacity and stability of the subgrade in some sections of the railway network. This is the situation we are dealing with right now on the Polish State Railways network. Therefore, as a case study, a fragment of an existing railway embankment based on a weak foundation was chosen for the analysis of train–track–subgrade interaction.

A two-stage train–track–subgrade model has been developed. The model consists of the upper part (train–track) and the lower part (subgrade-foundation). The first part is modelled as a self-contained system of differential equations which are solved by means of FDM which reveals the stress levels on the subgrade. These stresses are treated as the load for the lower system modelled using FEM. The model has been validated using experimental data from literature, the authors' measurements, and measurements of the track geometry conducted by railway staff. For numerical analyses, the results of geotechnical testing were used and vibration measurements were performed during passages of the Pendolino train in Poland.

Several cases of strengthening methods were calculated and compared with measurements on the railway section under consideration. Good agreement between the prediction and the measurement was found. The novelty of the model includes the heterogeneity of the subgrade, the strengthening methods, and very deep layers of its foundation as well as adding the influence of vibration on the weakening of soils. It was found that this influence is noticeable and should be included in the prediction of railway subgrade behaviour.

2 Subgrade stress levels and existing train–track–subgrade interaction modelling and measurements

The magnitude of the rail traffic action to be assumed during the modelling of subgrade bearing capacity is

given in several regulatory documents [1–3]. The range of the stress fields to be applied to the subgrade varies from approximately 20–30 kPa in the case of in-service objects to 20–60 kPa in the case of new and modernised objects. In this article, the stress levels are determined using the developed two-stage model.

As the literature review indicates, most of the train–track–subgrade interaction modelling is done by including the subgrade stiffness in the overall model of the train–track system. Such models are useful for predicting magnitudes of forces acting on the track due to the unevenness of the rail or abrupt stiffness changes along the track, which is the case with transition zones to engineering objects [4–9]. Another approach is based on analytical or empirical settlement models, which serve for predicting settlements of the track due to unevenness of the rail or spatial variations in track-bed stiffness (ballast + subgrade) [10–13]; this is especially covered in work in which the author summarised a dozen existing empirical formulas for track settlement prediction [14]. This kind of approach, although very useful, does not answer questions about the behaviour of the subgrade in deep layers.

Another approach is represented in other research [15,16] where realistic stress fields on top of the subgrade are determined and are then treated as loads for the deeper layers of the subgrade. In such papers, simplified subgrade models are usually employed in order to determine stresses in deeper layers of the railway embankment. For example, the Boussinesqmethod and its modifications [17] are used for ballast and subgrade layers without considering the effect of multi-layered structures. Other methods involve particulate-probabilistic theory or solutions with a multi-layered structure [18]. No strengthening methods are considered in such an approach.

A lot of work is devoted to determining admissible increased dynamic loads on the subgrade for the design purposes [19,20]; such work is usually accompanied by extensive laboratory or/and *in situ* measurements. Other papers [21,22] contain all important elements such as the realistic composition of the embankment and coupling of the track with the subgrade. In another paper [22], the authors propose a three-dimensional fully-coupled track–subgrade numerical model which was validated using deflectometers. These results are also used by the authors of this article for rough comparison with their own results.

The approach presented in this article is intended to be situated in the group of two-stage approach models of the train–track–subgrade modelling in which train and track are coupled and the subgrade (starting below the ballast layer) is uncoupled. An additional feature of the present model is that the authors take into account the heterogeneity of soils and strengthening methods of the railway embankment, which is a novelty. Additionally, vibration is added to the model to estimate its influence on the subgrade.

For the determination of stress levels on the subgrade, the authors use the results of previous research [23], which was performed on a conventional (ballasted) French railway line. These results are used for the validation of the proposed model. The measurements were taken at depths of 93 and 96 cm below the running surface of the rail. The results are shown in Figures 1 and 2 for the deflections and stresses accordingly. The service

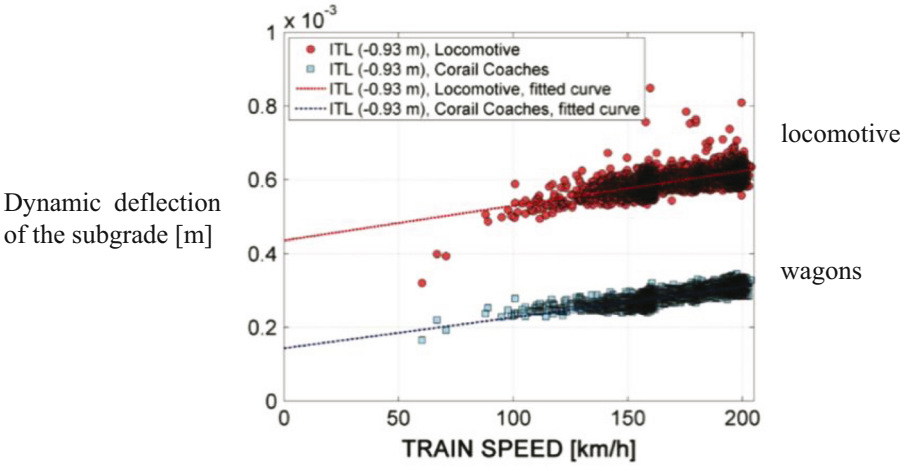

Figure 1: Amplitude of the dynamic subgrade deflection [23]; static locomotive axle load of 221 kN.

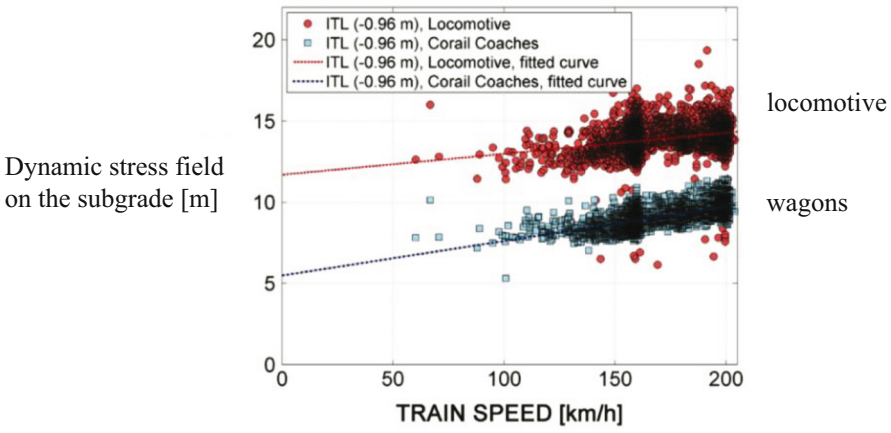

Figure 2: Amplitude of the dynamic subgrade stress field (normal to the surface of the subgrade [23].

parameters were the speed range of 50–200 km/h and the rolling stock was locomotives with 4 axles of 221 kN and cargo wagons with axle loads of around 180 kN. For further analysis, only the results obtained for the locomotives are considered.

As can be seen in Figures 1 and 2, the stress field is at a level of 12–14 kPa (Figure 2) and the corresponding subgrade dynamic deflections vary in the interval of about 0.4–0.6 mm – the linear regression lines (red lines) were taken for the locomotive. The results are consistent with the recommendations given in UIC Leaflet 719-R [24,25] for a subgrade in good condition.

It is noticeable that the magnitude of the stresses only slightly depend on the speed. If we calculated the speed factor in the range of 50–200 km/h, we would get roughly 14 kPa/13 kPa = 1.08. This result suggests that the subgrade works in semi-dynamic conditions, at least when it is in good condition and uniform along the track.

Rail deflection measurements are important for validation of train–track models. Some measurement methods, including the author's own, are described in the literature [26–29]. A new method of dynamic track stiffness measurement has been developed on the basis of a so-called falling weight deflectometer (FWD) with the load applied to the rail [27,28]. It is intended to be used for the validation of the extended two-stage model.

3 Model of the train–track interaction and its validation

A train–track model is presented below. The model described in Section 3.1 is self-contained and enables the determination of stresses at the bottom of the ballast. Next the stress levels obtained are treated as the load applied to the uncoupled, separately developed subgrade model, which is covered in Section 3.4. The whole two-stage model is applied to the analysis of a real cross section through the subgrade and its foundation as a case study (Section 4). An analysis of several cases is carried out in Section 5. Vibration is then added to the model on the basis of available data and one of the calculations is repeated in Section 5.4.3.

3.1 Applied model of the train–track interaction

The physical model is shown in Figure 3 and is composed of equation (1). The model consists of the Bernoulli–Euler beam resting on a linear foundation with viscous damping. The symmetry of the track in the cross section and continuous support are assumed. The foundation is a single layer

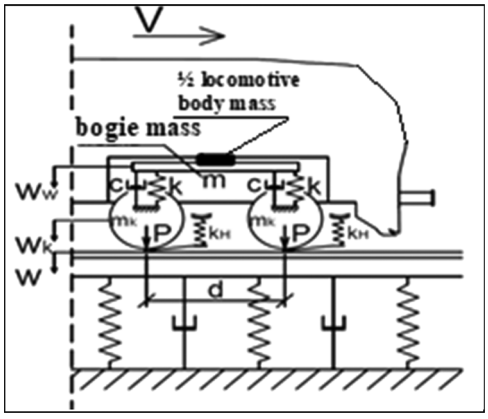

Figure 3: Vehicle-track model.

with stiffness for each support and damping parameters representing the rail pad, the ballast, and the top layer of the subgrade. The wheel suspension consists of a linear spring and a viscous damping element. The contact force between the wheel and the rail is modelled as a so-called Hertzian spring.

The equations are solved using the finite difference method (FDM). In previous research [30], the FDM solutions were compared with other analytical and numerical models (FEM) and good agreement was found. The novelty in these equations is the variability along the track with regard to support stiffness, damping coefficient, mass of the track beam, and the bending stiffness of the beam.

$$\begin{cases} (m_w + 1/2m_n)\ddot{w}_w + 2c \cdot \dot{w}_w + 2k \cdot w_w \\ \quad = c(\dot{w}_{k1} + \dot{w}_{k2}) + k(w_{k1} + w_{k2}) \\ m_k\ddot{w}_{k1} + k_H w_{k1} = k_H w_1 + c(\dot{w}_w - \dot{w}_{k1}) + k(w_w - w_{k1}) \\ m_k\ddot{w}_{k2} + k_H w_{k2} = k_H w_2 + c(\dot{w}_w - \dot{w}_{k2}) + k(w_w - w_{k2}) \\ E[I(x)w'']'' + Nw'' + U(x)w + m_s(x)\ddot{w} + c_t(x)\dot{w} \\ \quad = k_H(w_{k1} - w_1)\cdot \delta(x_1 - vt) + k_H(w_{k2} - w_2) \\ \quad\quad \cdot \delta(x_2 - vt), \end{cases} \quad (1)$$

where x – coordinate along the track, x_1 and x_2 – positions of the wheels, w_w – vertical displacement of the bogie (no rotations), w_{k1} and w_{k2} – vertical displacements of the wheels, w – rail deflections $w^1 = w(x_1)$ and $w^2 = w(x_2)$, m_n – mass of ½ of locomotive body at the bogie torsion pin, m – mass of one boogie, m_k – mass of one wheel set, c – damping coefficient of suspension, k – primary suspension stiffness, k_H – Herzian spring stiffness, $m_s(x)$ – unit mas (mass of one rail plus mass of ½ sleeper per 1 m of the track), E – Young's modulus of rail steel, $I(x)$ – moment of inertia of the rail (which may vary along the track), $U(x)$ – stiffness parameter of the foundation, $c_t(x)$ – viscous damping parameter of the rail support, N – longitudinal force in the rail, $P_i = k_H(w_k^i - w^i)$ – wheel–rail interaction force $i = 1, 2$, d – axle spacing in a bogie, δ – Dirac delta, which in numerical calculations is replaced with a continuous load applied on a very short section of the rail.

3.2 Validation of the train–track model

An example of validation of the model using measurements of rail deflections on a line in service in Krakow is shown in Figure 4. Rail deflections were measured using a geodesic method under a ballast-carrying wagon TMS. The parameters of the wagon are presented in Table 1 and the results of track stiffness measurements are shown in Table 2. The results of validation are shown in Figure 5.

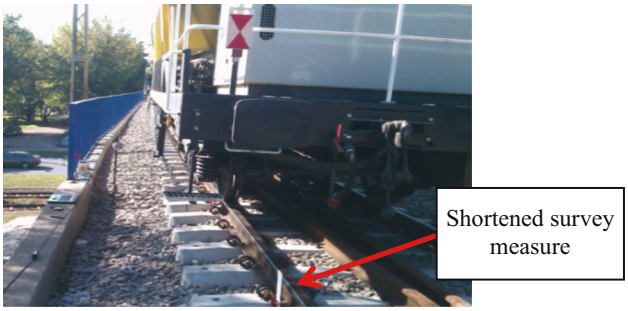

Figure 4: Geodesic measurements of rail deflections under a ballast-carrying wagon.

Table 1: Mechanical parameters of one bogie (per ½ track) – wagon TMS

Parameter	Notation	Data for 1/2 axle
Static wheel load (TMS wagon)	P	110 kN
Mass of one bogie (*)	m	5,000 kg
Mass of a wheel set (*)	m_k	1,180 kg
Primary suspension stiffness (*)	k	2,240 kN/m
Damping coefficient of suspension (*)	c	60 kN s/m
Axle spacing	d	1.8 m
Herzian stiffness	k_H	10^6 kN/m

(*) estimated values.

As a result of the measurements, the maximum deflections under axles were obtained, which were then corrected by "separation" of the second axle using an iterative procedure. This was performed using a model of a beam on an elastic foundation. In the procedure, two axles were assumed and the load magnitude corresponded to the axles given in Table 1.

Using this classical method, the static stiffness of the track was estimated with an accuracy of 0.1 mm. The

Table 2: Variability of rail foundation stiffness along the track

Position of measurement coordinate	Coordinate along the track (*) [m]	Stiffness U_i [MN/m^2]	
		North side	South side
Object	−2.0	45.36	68.74
Transition zone	1.0	60.72	73.48
Transition zone	4.0	58.96	64.51
Transition zone	7.0	60.72	48.82
Transition zone	10.0	45.36	52.76
Transition zone	13.0	38.77	50.07

(*) – coordinate "0" marks the beginning of the object.

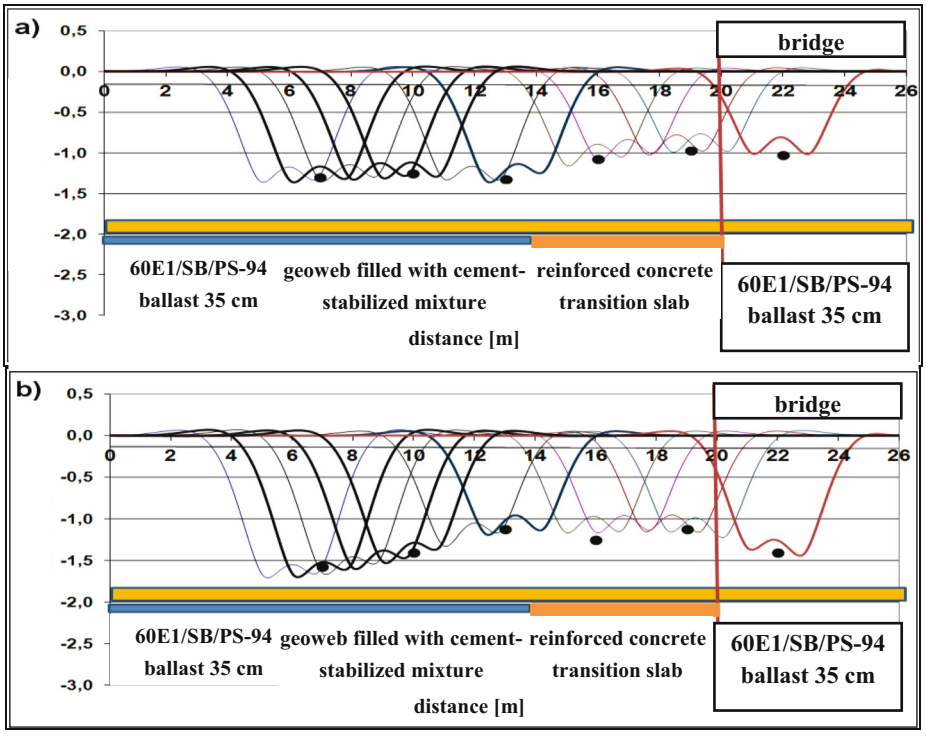

Figure 5: Calculated rail deflection lines in the transition zone compared with the measurements of rail deflections (denoted by dots): (a) north side of the object and (b) south side of the object.

error grows when the non-uniformity of the track stiffness is significant. In the case of dynamic deflection measurements as obtained in ref. [28] using the magnetic induction method, the values were similar.

The results of the comparison between the measured deflections (denoted by dots) and the calculated deflection lines are shown in Figure 5a and b. Due to the fact that the speed limit on the line was 80 km/h, the authors used this speed in the numerical calculations. The damping coefficient of the track $c_t(x)$ is assumed as zero due to the small influence of the speed. All other parameters are shown in Table 2 and the track structure 60E1/SB/PS-94 is shown in the Figure 5.

3.3 Data for the train–track modelling

For the purpose of the present calculations, locomotive TRAXX was used (Figure 4), the mechanical parameters of which are given in Table 3. A good parameter study of various trains is given in the literature [31]. In this context, it is sufficient that this locomotive has similar characteristics to that which was run on a section of a French line in which the stresses and the deflections were measured [23]. Therefore, the obtained stress fields, when compared to those measured, may be treated as a realistic estimation of the load on the subgrade (Figure 6).

The track parameters are as follows:

- 60 E1 rail;
- static stiffness of rail pad k_b = 32 kN/mm;
- twin-block sleeper U-41 (Figure 7) – length = 2.4 m, support area = 0.437 m², sleeper mass = 225 kg, and

Table 3: Traxx locomotive parameters assumed for model validation [32]

Parameter	Notation	TRAXX bogie (Number of axles 2)
Static axle load (*)	Q	221 kN
Mass of half of the body	m_n	29,100 kg
Mass of 1 bogie	m	10,000 kg
Mass of a wheel set	m_k	3,000 kg
Primary suspension stiffness	k	1,636 kN/m
Damping coefficient of suspension	c	27 kNs/m
Axle spacing	d	2.600 m
Maximum speed	v	200 km/h
Herzian spring stiffness (per axle)	k_H	2×10^6 kN/m

(*)$P = 1/2Q$ (static axle load).

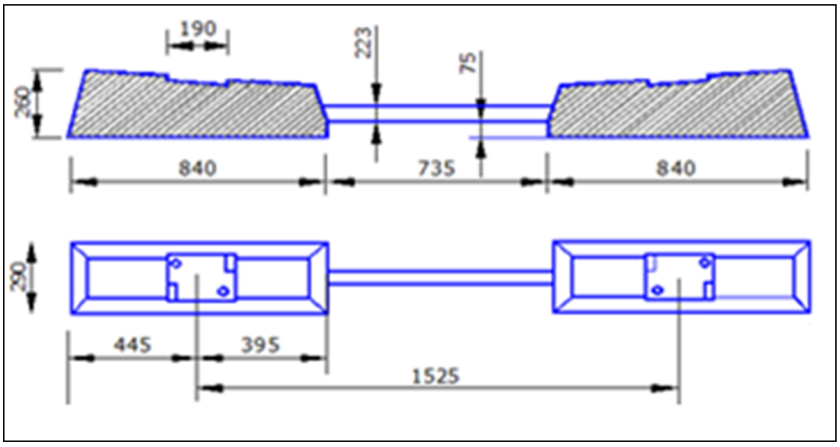

Figure 6: Twin-block sleeper U-41.

sleeper spacing = 60 cm, thus its support stiffness k_s = 68 kN/mm (half of the sleeper);
- ballast layer = 45 cm;
- the subgrade modulus is 75 MPa, next using the assumed stress distribution angle of 22° [33,34] and the sleeper dimensions, the stress area for the uniform distribution of stresses is obtained as 0.761 m², which with the stiffness modulus C = 150 MN/m² [35] yields the substitute stiffness for the foundation k_{sub} = 0.761 × 150 MN/m² = 114 kN/mm;
- stiffness of the three layers is determined according to ref. [36], $k_{track} = 1/(1/k_b + 1/k_s + 1/k_{sub})$ = 18.28 kN/mm;
- if this stiffness is distributed uniformly for a sleeper spacing of 0.6 m, the foundation stiffness parameter is $U = k_{track}/0.6$ = 30.5 MPa.

The mass of the rail including half of the sleeper per one meter of the track is m = 60 kg + 225 kg/2 × 1/0.6 m = 248 kg/m. The parameters assumed for calculations are shown in Table 4. Generally, the parameters correspond to those provided in the literature [37,38].

On the basis of the calculations of the deflection lines, the reaction per half sleeper was determined as 31.5 kN, and next the stresses at the bottom of the ballast was determined assuming the stress distribution angle in the ballast as 22° [34,39]. Thus, they are equal to 34 kPa. These stresses further spread in the subgrade, and at the level of 95 cm below the running surface of the rail, they reach a value of 23 kPa. They are 30% larger than those measured in previous research [23]. This may be attributed to the larger stress distribution angle assumed in the latter work.

3.4 Numerical model of the ballast-subgrade system and its validation

In order to make sure that the stress levels in the numerical model of the subgrade are correctly determined, the upper part of the subgrade is first modelled. For this purpose, a 2D FE model was developed in program MIDAS GTS NX. The calculations were performed according to the guidelines given in the Eurocode [33] assuming the sleeper loads as the reaction forces obtained from the numerical train–track model in Section 3.2. The soil

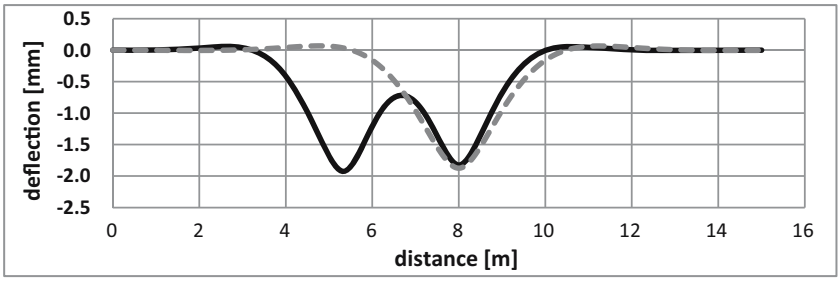

Figure 7: Calculated deflection lines for the track as the first stage of the model. The data are given in Table 4, and the speed is 200 km/h. Deflection under 1st axle is 1.74 mm, deflection under 2nd axle is 1.88 mm, and in the case of one axle, the deflection is 1.81 mm.

Table 4: Parameters of the track structure for calculations

Parameters		Values
Bending stiffness (60E1 rail)	EI [MN m^2]	6.42
Mass of the beam per 1 m of track	m_b [kg/m]	248
Foundation stiffness	U [MPa]	30.5
Viscous damping coefficient (*)	c [kN s/m^2]	100

(*) assumed on the basis of the review performed in the literature [30].

Table 5: Parameters of the ballast, blanket layer, and the subgrade for the comparative calculations

Layer	E [MPa]	E+ (*) [MPa/m]	φ [deg]	Cohesion [kPa]
Ballast	80	60	22	0
Blanket layer	80	60	25	0
Subgrade	45	63	32	1

(*) increase in the value with the depth of the model (bi-linear stiffness characteristics).

parameters are shown in Table 5. The results of the validation of this model and the numerical train–track model are summarised in Table 6 (Figures 8 and 9).

Additionally, in order to compare the stress values discussed above, the laboratory tests described in the literature [34,39] are quoted. There, the ballast was carefully compacted and its depth was 32 cm. At the bottom, special measurement plates were put underneath the ballast layer which measured the stresses while the load wads were applied (statically and dynamically). As can be seen in Figure 10, the distribution of the stresses is not uniform.

The vertical load was correlated to the possible reaction per sleeper in service conditions. It was equal to 41 kN per fastening system. The measured stresses were around 30 kPa in the area directly under the fastening system (area 1 in Figure 10).

In summary of Section 5, it may be stated that the validation, comparative calculations (Table 6), and tests [39] indicate that the stresses determined using the models developed in Section 3 are a good representation of the track behaviour. The subgrade deflections shown in Table 6 and obtained using a numerical ballast-subgrade model (0.59 mm) are convergent with the results of measurements in a previous research [22] for a similar locomotive. The comparative calculations and the validations are proof that the model parameters and their structures are correct and may be justly used for the subgrade and its foundation modelling in Sections 4 and 5.

4 Mechanical parameters of the ballast and soil layers in the calculations of the subgrade foundation

The second stage of the model – the subgrade and its foundation – is modelled numerically using the geotechnical data from geotechnical tests [37]. The cross section through the site of the critical embankment is shown in Figure 11. Geotechnical soil parameters are given in Table 7. Several cases of strengthening methods were

Table 6: Results of the comparative calculations and validation

Value	Measurements [23]	Numerical train–track model [Section 3.1]	Numerical ballast-subgrade model [Section 3.4]
Rail deflection	x	1.88 mm – second axle 1.74 mm – first axle one axle case: 1.81 mm	X
Fastening deflection	x	x	X
Reaction of 1 sleeper per rail	x	32.1 kN	Load as reaction forces
Sleeper deflection	x	x	0.44 mm
Subgrade deflection (–0.70 m)	x	x	X
Subgrade deflection (–0.95 m)	0.4–0.6 mm	x	0.59 mm
Under sleeper stress	x	x	X
Subgrade/ballast stress	30 kPa	34 kPa	30 kPa
Stress at –0.95 m level	15–18 kPa	23 kPa	26 kPa

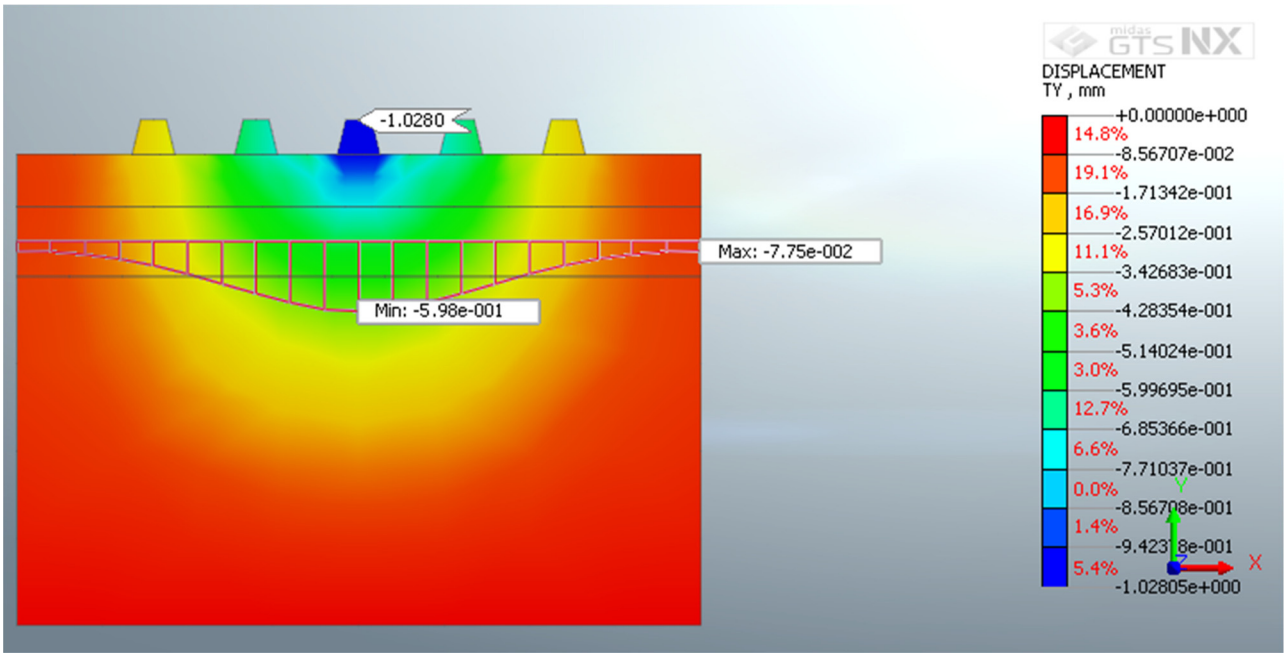

Figure 8: Vertical displacement map (Ty), [mm] – the sleeper deflection here is 1.03 mm (which is the sum of ballast deflection of 0.44 mm and subgrade deflection of 0.59 mm at the level of 95 cm below the running surface of the rail).

modelled and compared with the authors' own observations and with the help of settlement measurements performed by railway staff.

From the geotechnical test, it follows that the oedometric moduli of the soils that compose the analysed structure are very different: for sands (yellow), oedometric moduli vary within the range of 5–135 MPa, while for slits (green), they are very low – they reach a maximum of a few MPa. The internal friction angles for cohesive soils vary in the range of 27–35°.

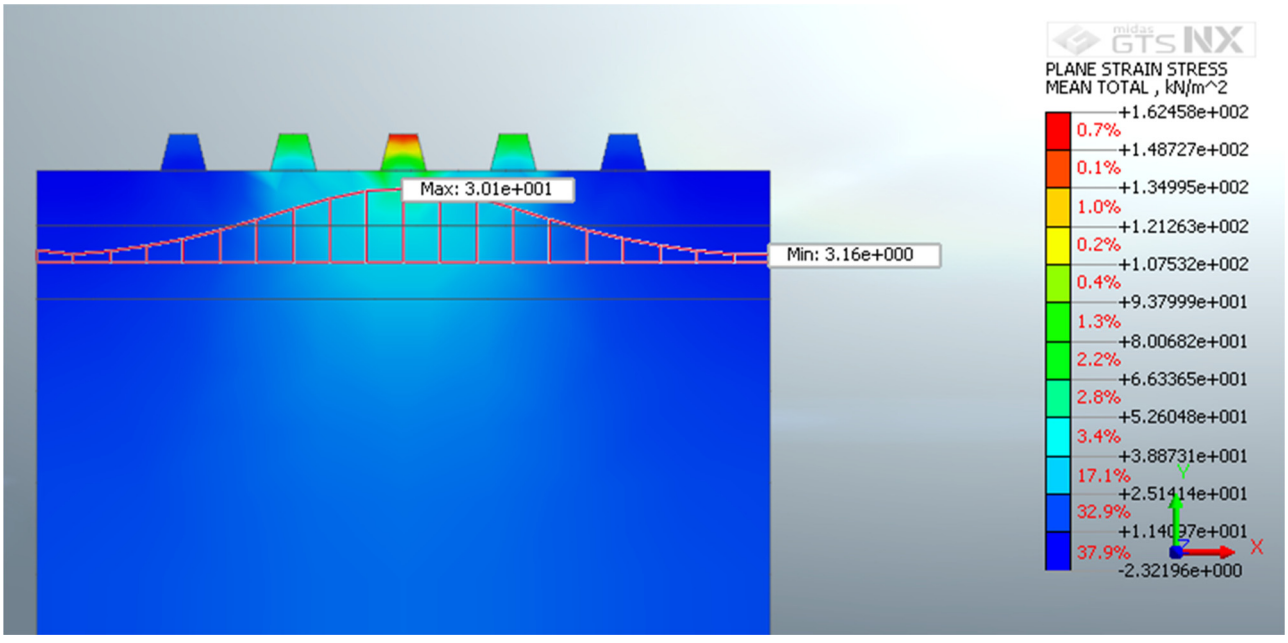

Figure 9: Vertical stress distribution [kPa] – maximum value of 30 kPa at the level of 95 cm below the running surface of the rail.

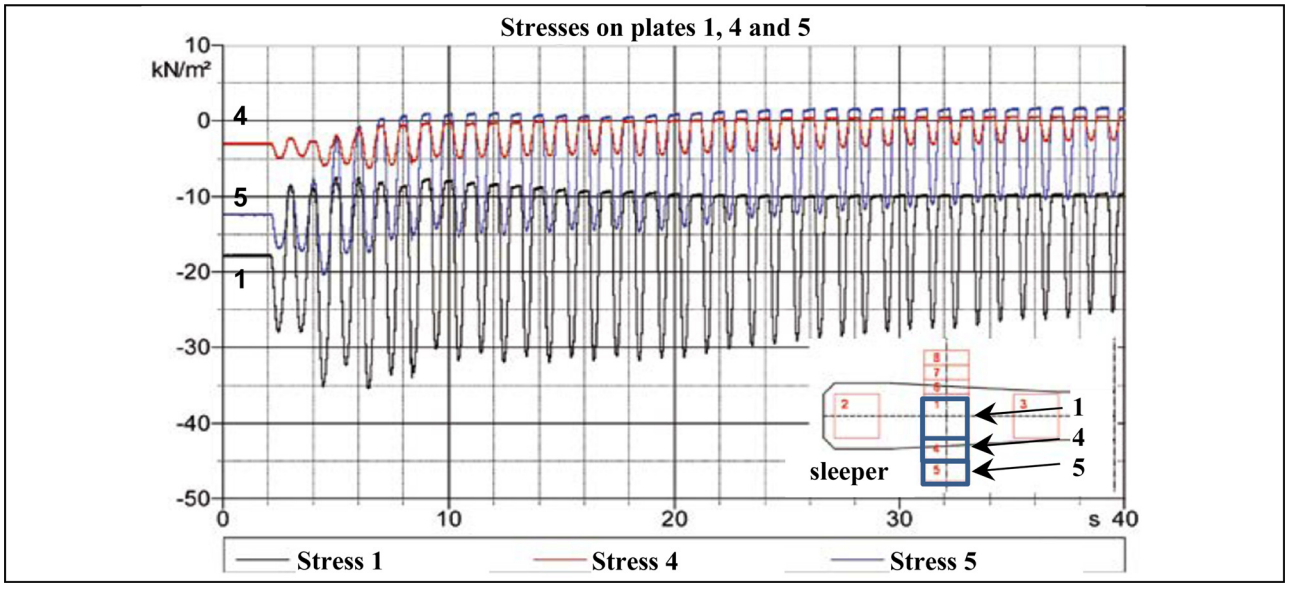

Figure 10: Distribution of the vertical (normal) stresses underneath the ballast layer [39].

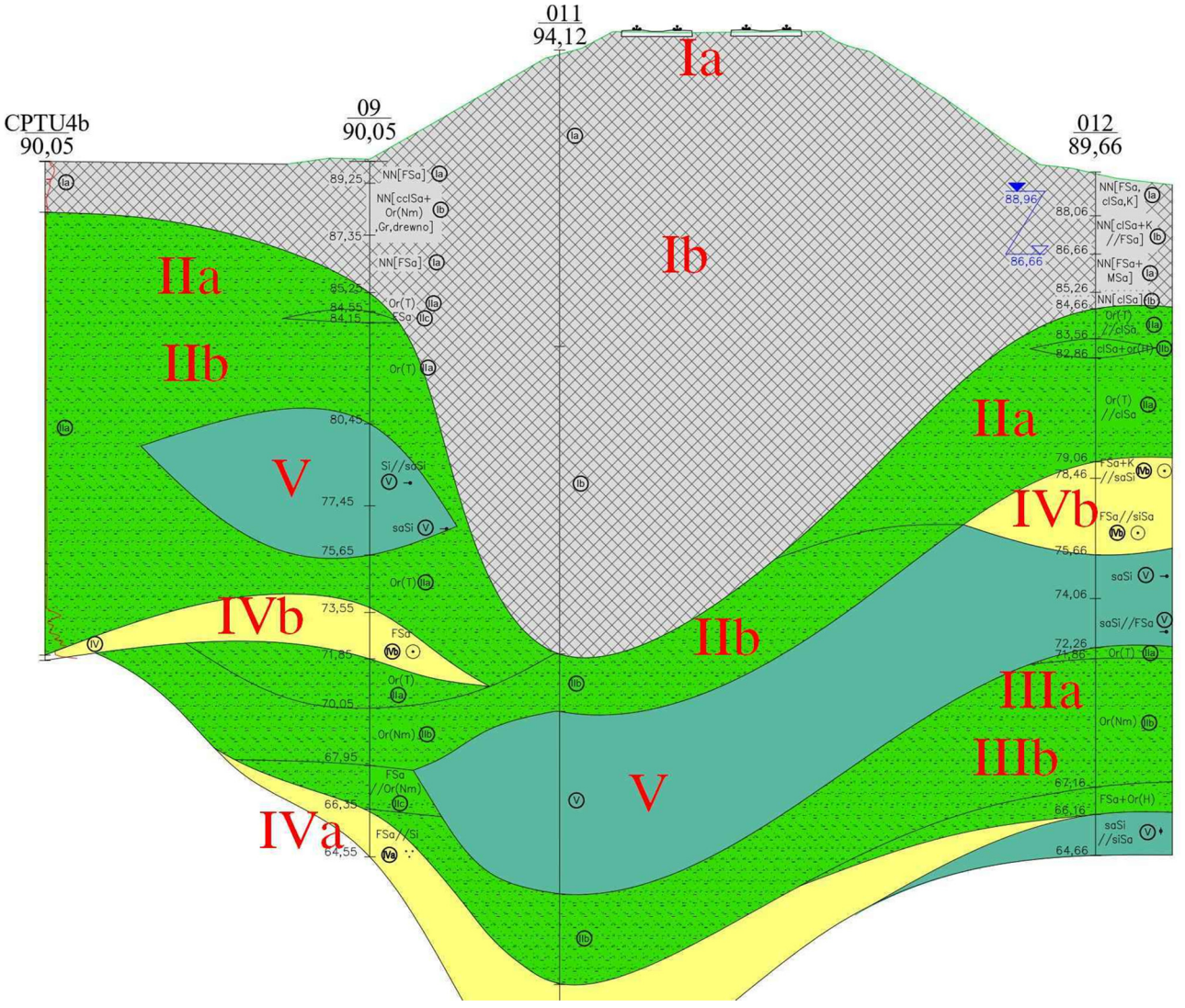

Figure 11: Geotechnical cross section through the embankment and its foundation. The depth of the tests exceeded 30 m. Green denotes organic soils, grey – anthropogenic soils, yellow – non-cohesive soils, and blue – cohesive soils.

Table 7: Soil parameters used for numerical calculations

Layer	ϕ [deg]	c [kPa]	E [MPa]
Ia	28.8 (25.9*)	0	18,000 (15,560*)
Ib	14	11.3	11,500
IIa	3.4	8.5	1,500
IIb	7.2	6.8	1,000
IIIa	5.5	99	1,800
IIIb	14.5	22	15,000
IVa	29.5	2	29,700
IVb	32	1	45,000
V	19	19.5	21,000

Note: *parameters weakened due to vibrations (see discussion in par. 5.4).

5 Analysis of selected methods of the subgrade and its foundation strengthening

Two methods of strengthening were analysed on the "background" of the case without any strengthening – the result of the calculations is shown in Figure 12. The load was applied to the top layer of the subgrade as a stress field calculated from the train–track model.

As the first method, a palisade was used at the foot of the embankment (continuous flight auger piles). The palisade was finished with a reinforced concreate cap (a beam which was connected to the heads of the piles) along the embankment. Next the palisades on both sides were connected with tie-rods which were lead through the embankment. The result of the calculations is shown in Figure 13.

The second method consisted of replacing the soils that are located in the centre of the embankment with cohesive soil at a depth of up to 2.0 m and installing vertical reinforced concrete piles in the centre of the structure. At the bottom, these piles reached the soil layers of high bearing capacity and were finished with a special mattress at their heads in order to better distribute the load. The result of the calculations is shown in Figure 14.

5.1 Embankment prior to strengthening

On the basis of the calculations, it is concluded that the maximum settlement will reach 278 cm, which is unacceptable. This is due to the fact that the foundation of the embankment is very weak, so the self-weight of the soil mass above the foundation is dominating the behaviour of the structure.

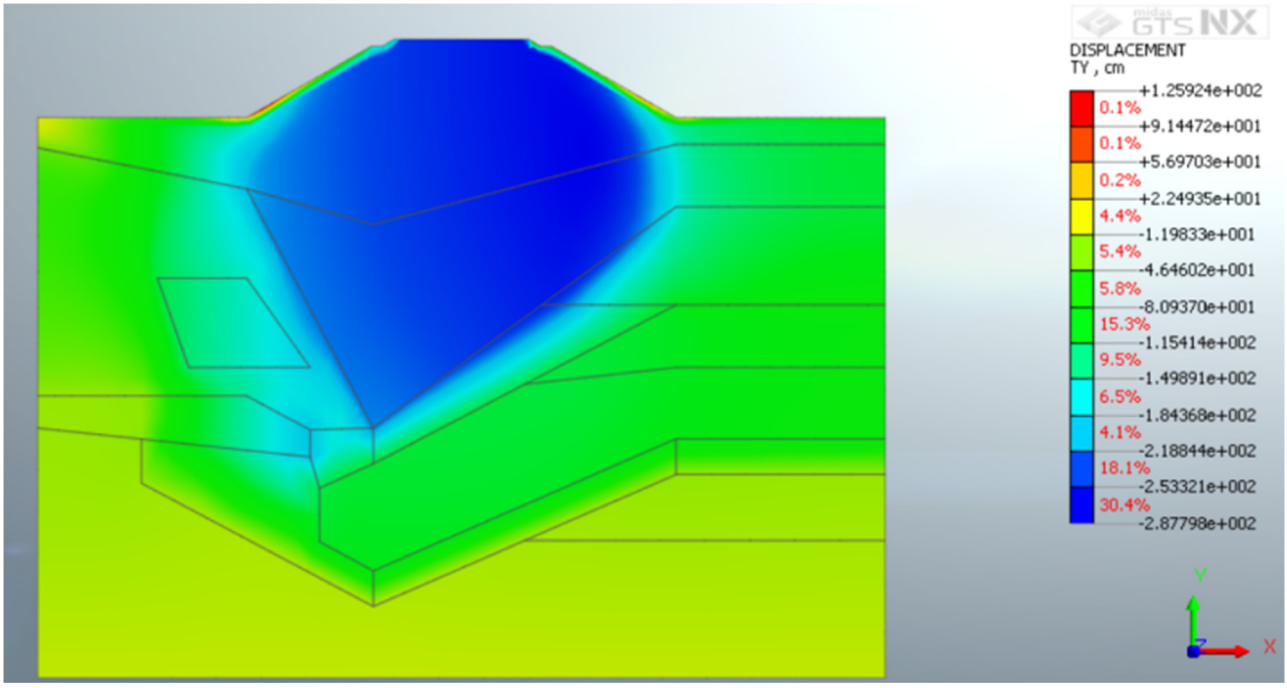

Figure 12: Vertical displacement map prior to strengthening.

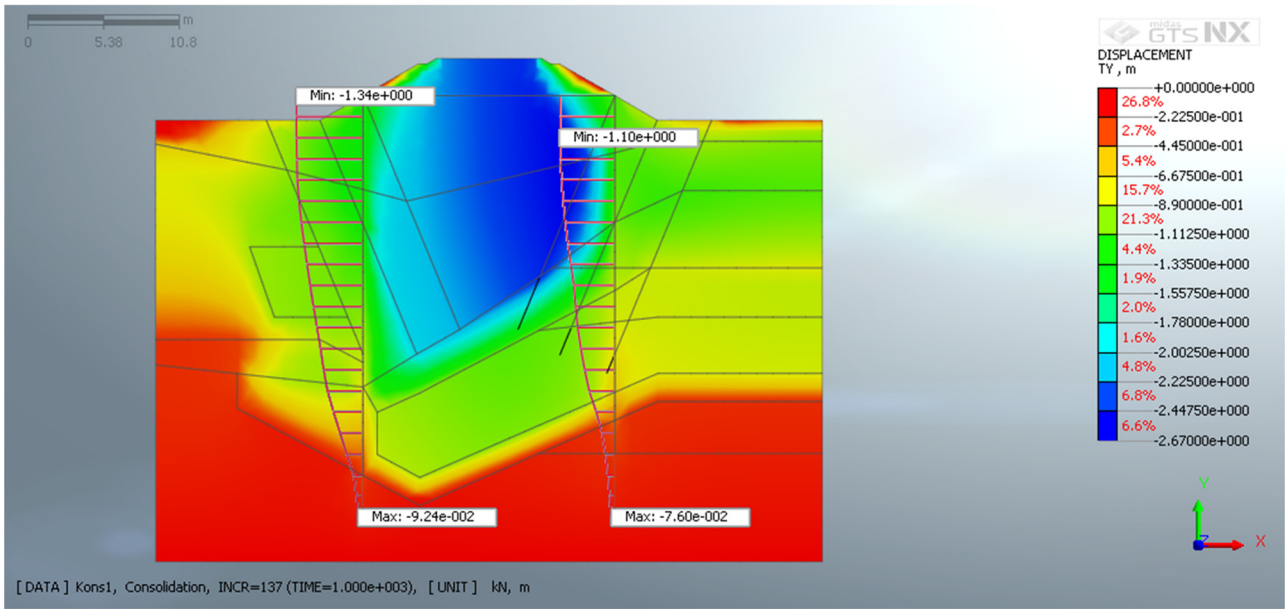

Figure 13: Vertical displacement map after strengthening.

5.2 Embankment after strengthening with palisades on both sides

The calculations of this case showed that the maximum vertical settlements reach 267 cm, which is not a significant improvement in relation to the previous case. Such behaviour of the structure indicates that the main component of the settlement is the foundation – the whole embankment settles as approximately one block.

5.3 Embankment after strengthening with palisades on both sides and piles placed in the centre

In this case, the calculated maximum settlement was 3.0 cm. This result is satisfactory from the point of view of the regulations. To be complete, the calculation should also include checking the gradient of settlements along the embankment to identify whether it exceeds admissible values. This is omitted here as it is irrelevant for the purpose of the article.

5.4 Embankment with weakened soils due to train-induced vibration

In this case, the structure was identical to that given in Section 5.2, but it was additionally weakened by the influence of vibration that propagates in the soils. The parameters of the soils in this case will be reduced following the findings of the research performed by Cracow University of Technology during test runs of the Pendolino train [40].

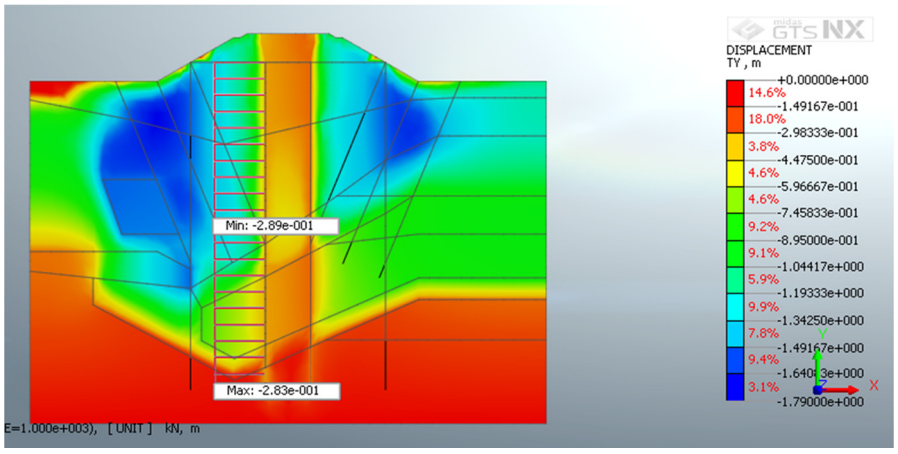

Figure 14: Vertical displacements map after strengthening with palisades on both sides and piles placed in the centre.

Research concerning vibration propagation into the subgrade and the environment has been the subject of a great number of papers. The analyses were made from the point of view of the transmissibility of vibration through soils, strain waves, or vibration mitigation [41]. A summary of research is given in the literature [42]. Natural frequencies of soil layers and resonance phenomena have also been studied [43,44]. However, the problem of the influence of vibration on the soil-bearing capacity of railway subgrades had not yet been fully analysed; therefore, this was undertaken by the authors. The question arises of how a speed increase on a line – which means higher accelerations and amplitudes of vibration – influences subgrade settlements and the formation of track unevenness.

Some data concerning this issue is provided in the literature. As a result of the vibration, the internal friction angle is reduced, which means a loss of strength. In the case of cohesive soils, the cohesion coefficient is also reduced. In the literature [45] it was noted that accelerations of soil particles at some critical level change the state of the soil, which leads to plasticisation and an abrupt loss of strength. The author tested ground samples (granular soils) under various stresses, amplitudes, and frequencies of vibration. For example, as a result of vibration action in the order of 140–250 Hz, the soil particles exhibited compaction in the order of 20% in relation to the sample height. This compaction remained after the vibration action was stopped, but the shear strength was restored to its original value. The total strength loss of granular soil (coarse sand) during vibration action was determined at 13% at a vertical acceleration of 0.1 g, and reached 22% at an acceleration of 0.145 g. The particle displacement amplitude was in the range of $(1.0-1.5) \times 10^{-3}$ mm. The reduction in the friction angle was found to be at a level of 10%.

In the literature [46], a vibration loss coefficient was proposed. This coefficient was proposed to be a measure of the influence of vibrations on soil strength. This would result in the change in the oedometric compression modulus of the soil.

In the present calculations, the above strength loss was assumed in the oedometric moduli of the non-cohesive soils (which is 13%) and the friction angle was reduced by 10%, since such an order of magnitude was found in the quoted research. The reduced parameters are shown in Table 8. It has been assumed in these calculations that this loss in the internal friction angle is independent of the normal stress in the soil. At present, the authors have left out the problem of the possible plasticisation of soils in the foundation of the embankment.

Table 8: Soil parameters used for the simplified model of vibration decay

No.	Notation	Unit	Value
1	p	kg	3,270
2	ν	—	0.225
3	G	kN/m²	7,500–12,500
4	D	—	0.05
5	ω	rad/s	727
6	v_s	m/s	270

5.4.1 Research into vibration propagation during tests with the Pendolino train

The measurements of vibration propagation were made by a team mainly comprised of University researchers in 2014 [40]. The measurements were made on the main line at various train speeds and with a top speed of 293 km/h (speed record on the Polish railway network). Curves of the vibration decay are shown in Figure 15.

The results of the research show that there is a linear relationship between the speed of the train and the accelerations of sleepers. These accelerations propagate to the ballast and are approximately 10 times smaller next to the track (but still on the top of the subgrade). They decay very quickly at the foot of the embankment, and at some distance from the embankment, they became indistinguishable with regard to the train type. The order of magnitude of the accelerations is 80–90 cm/s² (approximately 0.1 g) and at the foot of the embankment (which was about 6 m high), it is 5–20 cm/s² (about 0.02 g). These results justify use of the aforementioned rates of strength losses of soils because they correspond to the range of amplitudes and frequencies in the quoted paper [45].

5.4.2 Model of vibration decay in soils

For the purpose of the present article, the authors use a simplified model of vibration decay in soils with the assumption that the foundation is an elastic half-hemisphere [44]. This simplified model is as follows:

$$u(r,f) = \frac{p(1-\nu)}{2\pi\, G\, r} e^{-\mathrm{Dr}\star}, \tag{2}$$

where, $u(r,f)$ – amplitude of vibration (mm), r – distance from the source (m), f – frequency of vibration (Hz), p – vertical service load (reaction per half sleeper) – Table 8, ν – Poisson ratio of the soil – Table 8, G – shear modulus of the soil – Table 8, D – damping coefficient of the soil – Table 8, $r\star = \omega r / v_s$ – dimensionless coefficient of the

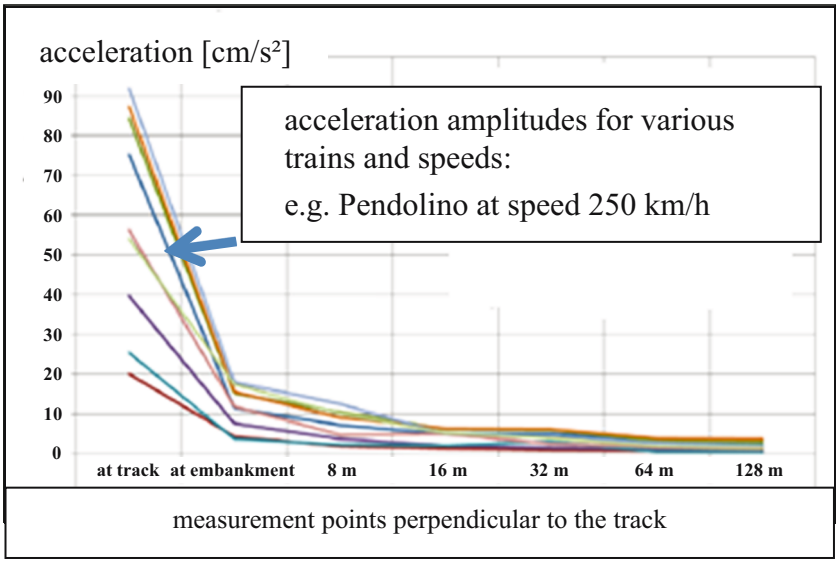

Figure 15: Vibration decay as measured by sensors placed on a line perpendicular to the track, the maximum distance is 128 m and the curves represent various trains that passed the site – the curve for the Pendolino is indicated by an arrow [40]. Other lines are obtained for lower speeds starting at 60 km/h and for other types of trains, which is less important for the present article.

distance from the source of vibration, ω – angular frequency of vibration – Table 8, v_s – speed of vibration-wave propagation in the soil – Table 8.

Examples of vibration decay plots are shown in Figure 16. The data for the calculation are presented in Table 8. Assuming small strain theory and taking the linear relationship between the compressibility modulus and the shear modulus $G = E/2(1 + \nu)$, which for layers Ia and Ib (Table 7) means that E belongs to interval 12,000–18,000 kPa, one obtains the average shear modulus G = 6,000 kPa. The Poisson ratio was assumed as average for gravel, coarse sand, and fine sand which is ν = 0.225 [47]. In the calculations that follow, two layers were considered for the purposes of comparison: layer Ia with E = 18,000 kPa and layer IVa with E = 29,700 kPa. These values correspond to shear moduli G = 7,500 kPa and G = 12,500 kPa, respectively. The damping coefficient of the soils was assumed as being constant at D = 0.05 and the shear wave propagation was v_s = 270 m/s [44] for gravel and sands.

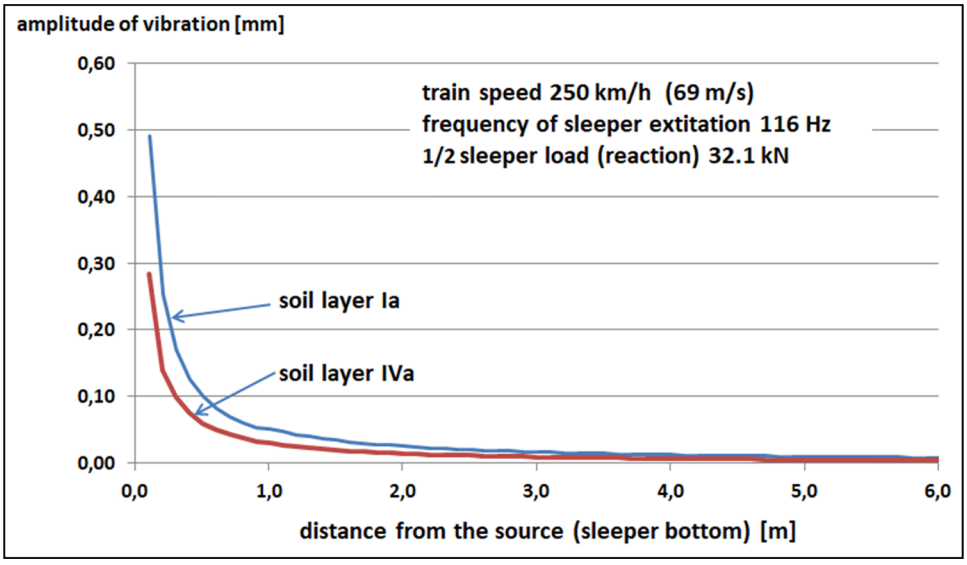

Figure 16: Dependence of the vibration amplitude on the distance from the source (sleeper bottom) on the basis of ref. [44].

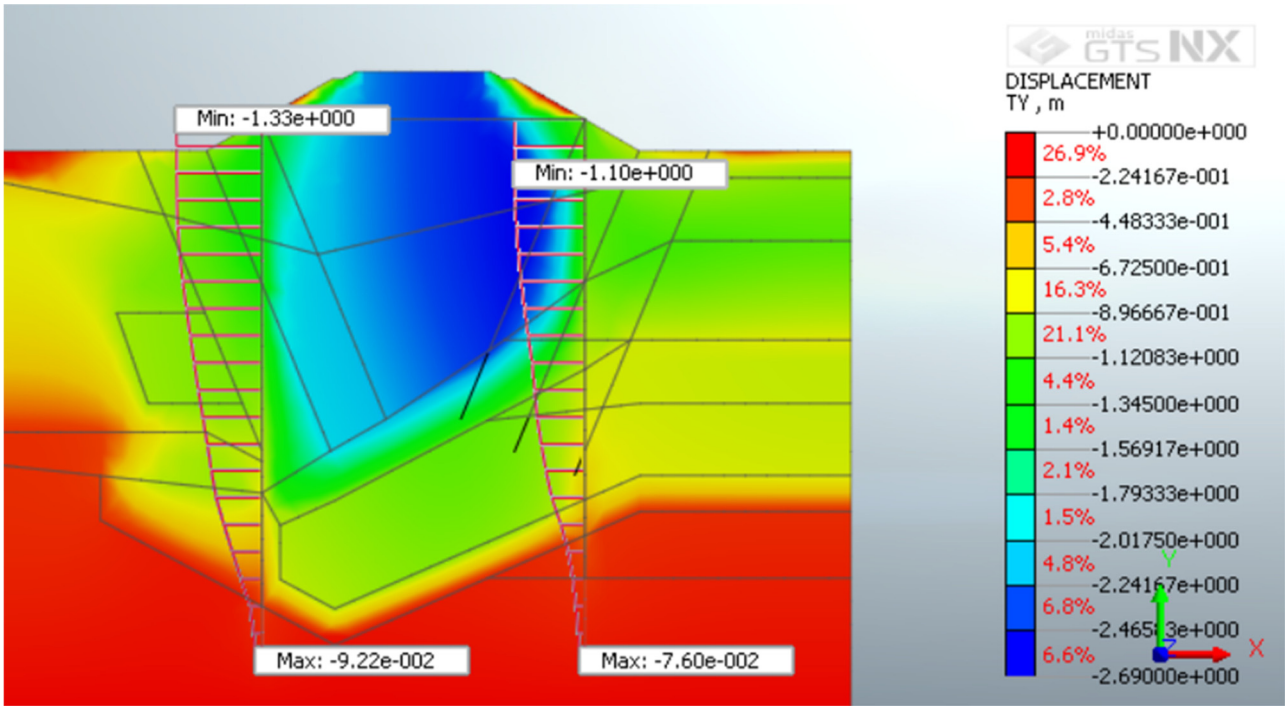

Figure 17: Vertical displacement map of weakened soils with the weakening effect.

For the following calculations, the speed of the train was 250 km/h (69 m/s) as in Figure 15. The decay curve is similar to that obtained for a classic train with a locomotive at a speed of 160–200 km/h. The load was treated as the reaction force underneath the sleeper (per rail) (denoted by p = 32.1 kN as in Table 6 and equal to 3,270 kg). The frequency was calculated from the sleeper excitation as the speed of the train/sleeper spacing, which gives 69 m/s/0.6 m = 116 Hz, and the angular frequency was 727 Hz.

In Figure 16, we can observe that the vibration amplitude at the bottom of the sleeper (distance close to zero) is within the range of about 0.3–0.5 mm, which is a realistic estimation and this is convergent with the calculated sleeper deflections in the track model and the FEM soil model (Table 6).

5.4.3 Calculations of the embankment settlements with soils weakened due to vibrations

The last calculation example is comparable to that in Section 5.2; however, this time the soils were weakened as shown in Table 8. The results are presented in Figure 17.

The results of the calculations shown above do not at this point indicate a significant difference in the settlements between the weakened and not weakened cases. However, some effect can be seen in the form of a difference of around 10 mm.

6 Conclusion

The approach to modelling the train–track–subgrade system presented in this article can be classified in a group of two-stage models with the coupled train–track model and the decoupling of the subgrade and its foundation. The novelties of the model are the inclusion of the heterogeneity of the embankment and taking into account very deep layers of its foundation as well as the vibration-weakening effect.

Due to a lack of comprehensive measurements with regard to the track structure, the model parameters had to be taken from literature. Within the subgrade and its foundation, the authors used reliable geotechnical tests for modelling. A drawback of the model is that the subgrade and its foundation were analysed in one cross section (2D). An extension to 3D is necessary to fully use the advantages of the train–track model in order to model the development of settlements along the track.

On the basis of the comparisons between the calculated displacements and stresses and those obtained from experimental research (both laboratory [34,39]

and field measurements [23]), it may be stated that the calculated results and measurements are convergent. This means that the model is validated. Similarly, the calculated settlements of the embankment (the existing state and the strengthened state using the palisade) agree with those settlements measured on the object in 2018–2019 during the strengthening works [37].

With regard to the calculation examples, it has been shown that the only efficient solution to the settlement problem of this embankment is strengthening it using not only palisades but also piles in its centre which reach the bearing layers of the site. Such strengthening is not possible without stopping the traffic.

As far as the influence of the vibration on the weakening of soils is considered, it may be concluded at this stage that this influence has been found to be noticeable (10 mm difference). The estimated result should be refined using a more precise model of vibration influence on the soil parameters on the basis of complex data collected at one site. An improvement in the model is also needed for the organic soils which may exhibit a sort of "flow," which will have a devastating effect on the bearing capacity of the whole structure. Such an effect was observed on the track during a visual inspection of the object.

An extension of the model to 3D is planned with necessary measurements of the deflections, accelerations, and stresses in a real track in service. The use of the new FWD method for extended model validation is envisaged.

Conflict of interest: Authors state no conflict of interest.

References

[1] Regulation of the Minister of Infrastructure and Development, 5th June 2014 (Journal of Laws no. 867) (in Polish).

[2] PN-EN 15528: 2013. Railway applications – Line categories for managing the interface between load limits of vehicles and infrastructure.

[3] PN-EN 1991-2: 2007 Eurocode 1: Actions on structures – Part 2: Traffic loads on Bridges.

[4] Lei X, Mao L. Dynamic response analyses of vehicle and track coupled system on track transition of conventional high speed railway. J Sound Vib. 2004;271:1133–46.

[5] Wu XT, Thompson DJ. Theoretical investigation of wheel/rail non-linear interaction due to roughness excitation. Veh Syst Dyn. 2000;34:261–82.

[6] Wu YS, Yang YB, Yau JD. Three-dimensional analysis of train-rail-bridge interaction problems. Veh Syst Dyn. 2001;36(1):1–35.

[7] Jabbar-Ali Z, Ghorbani V. Investigation on dynamic behavior of railway track in transition zone. J Mech Sci Technol. 2011;25(2):287–92.

[8] Yu Y, Zhao L, Zhou C. A new vertical dynamic model for railway vehicle with passenger-train–track coupling vibration. Proc IMechE Part K: J Multi-body Dyn. 2020;234(1):134–46.

[9] Davis D, Plotkin D. Track settlement at bridge approaches: what causes track settlement at bridge approaches and how can railroad engineering departments deal with the problem safely and efficiently? Railway Track and Structures; New York City, USA: Simmons-Boardman Publishing Corporation, February 2009, www.nxtbook.com (access 21.04.2010).

[10] Frőling RD. Low frequency dynamic vehicle/track interaction: Modelling and simulation. Veh Syst Dynamics, Int J Veh Mech Mobil. 1998;29:30–46. doi: 10.1080/00423119808969550, Issue sup1, Published online: 27 July 2007.

[11] Frőhling RD, Scheffel H, Ebersohn W. The vertical dynamic response of a rail vehicle caused by track stiffness variations along the track. Veh Syst Dyn. 1996;Supplement, 25:175–87.

[12] Ferreira PA, López-Pita A. Numerical modeling of high-speed train/track system to assess track vibrations and settlement prediction. J Transp Eng. 2012;139(3):330–7.

[13] Grossoni I, Andrade AR, Bezin Y, Neves S. The role of track stiffness and its spatial variability on long-term track quality deterioration. Proc I Mech E Part F: J Rail Rapid Transit. 2019;233(1):16–32.

[14] Grossoni I, Powrie W, Zervos A, Bezin Y, Le Pen L. Modelling railway ballasted track settlement in vehicle-track interaction analysis. Transportation Geotech. January 2021;26:100433.

[15] Xu F, Yang Q, Liu W, Leng W, Nie R, Mei H. Dynamic stress of subgrade bed layers subjected to train vehicles with large axle loads. Shock Vib. 2018(5):1–12. doi: 10.1155/2018/2916096. https://www.researchgate.net/journal/Shock-and-Vibration-1875-9203.

[16] Wang H, Zeng LL, Bian X, Hong ZS. Train moving load-induced vertical superimposed stress at ballasted railway tracks. Adv Civ Eng. 2020(22):1–11, Article ID: 3428395, doi: 10.1155/2020/3428395.

[17] Tang C, Lu Z, Yao H, Guo S, Huang X, Liu J. Semianalytical solution for dynamic responses of railway track system on unsaturated poroelastic half-space subjected to moving trainload. Int J Geomech. March 2021;21(3):04021016. doi: 10.1061/(ASCE)GM.1943-5622.0001955.

[18] Kandaurov II, Mechanics of discrete media and its application to construction, Izd. Liter Po Stroitel'stvu, Russia, 1966 (in Russian).

[19] Liu G, Luo Q, Lv Y, Meng W, Chen H. Design load of high-speed railway subgrade structure. Proceedings of the Fourth International Conference on Transportation Engineering. Chengdu, China: October 19–20, 2013, doi: 10.1061/9780784413159.408.

[20] Zhang X, Zhao C, Zhai W, Shi C, Feng Y. Investigation of track settlement and ballast degradation in the high-speed railway using a full-scale laboratory test. Proc Inst Mech Eng, Part F: J Rail Rapid Transit. 2019;233(8):869–81.

[21] Savidis SA, Hirschauer R, Bode C, Schepers W. 3D simulation of dynamic interaction between track and layered subground. System dynamics and long-term behavior of railway vehicles, track and subgrade. Berlin Heidelberg: Springer-Verlag; 2003. p. 431–50.

[22] Mezeh R, Mroueh H, Hosseingholian M, Sadek M. Fully-coupled numerical model for ballasted track analysis – Field measurements and predictions. Transportation Geotech. March 2021;21:100483.

[23] Lamas-Lopez F, Cui YJ, Calon N, D'Aguiar SC, De Oliveira MP, Zhang T. Track-bed mechanical behaviour under the impact of train at different speeds. Soils Found. 2016;56(4):627–39.
[24] UIC 719 R. Earthworks and track bed for railway lines, UIC 2008.
[25] Requirements catalog for the construction of slab tracks, DB railway network, 2002 (in German).
[26] Sołkowski J, Lisowski S, Pawlak-Burakowska A, Jamka M. Outline of the methodology of stiffness measurements of the track and the subgrade in transition zones to engineering objects and on objects. Sci Technical Noteb Assoc Transp Eng Technicians. 2012;3(99):285–306 (in Polish).
[27] Sołkowski J, Siemieński D. Testing and evaluation of the stiffness of the railway structure using a new measurement method. All-Poland Railway Conference INFASZYN; 2018. Proceedings. p. 128–33 (in Polish).
[28] Sołkowski J. *Testing the dynamic stiffness of the railway track by the method FWD*, XVII All-Poland Scientific and Technical Conference Modern Technologies and Management Systems in Rail Transport Zakopane. Scientific and Technical Notebooks of the Association of Transport Engineers and Technicians. vol. 12; 2018. p. 95–102 (in Polish).
[29] Development and implementation of an innovative universal system for monitoring transition zones by the company NeoStrain Ltd., contract no.MRPO.02.02.02-12-2-0686-27-13, Cracow, 2014 (in Polish).
[30] Sołkowski J. Transition effect in rail tracks. Monograph Cracow University of Technology, habilitation thesis, Cracow; 2013 (in Polish).
[31] Klasztorny M, Szurgott P. Numerical multi-parameter simulation of the behavior of a complex bridge structure during running three types of trains P250 (DB), P300 (SNCF) and T120 (DB) and when adopting a transition slab or a ballestless track structure. Road and Bridge Research Institute: Warsaw; 2010 (in Polish).
[32] www.wikipedia.org/wiki/Bombardier_TRAXX (access 12.11.2013).
[33] PN-EN 1997-1: 2008 Eurocode 7: Geotechnical design Part 1: General rules.
[34] Steiner E, Kuttelwascher C, Prager G. Spread of pressure from loaded railway sleepers in the contaminated track ballast. ETR Austria. 2014;6:68–72 (in German).
[35] Jankowski W, Sołkowski J. Research on transition effect in transition zones at engineering structures – an example of object founded in difficult conditions. Monograph Contemporary Challenges in the Design of Road and Rail Infrastructure, Cracow; 2021 (in Polish).
[36] Kerr AD. On the determination of the rail support modulus k. Int J Solids Struct. 2000;37:4335–51.
[37] Geotechnical tests, Polish State Railways (PKP PLK S.A.) 2018-2019 (in Polish).
[38] Knothe K. Benchmark test for models of railway track and vehicle/track interaction in the low frequency range. Veh Syst Dyn. 1995;Supplement 24:363–79.
[39] Steiner E, Kuttelwascher C, Prager G. Spread of pressure from loaded railway sleepers in track ballast. ETR Austria. 2012;12:71–5 (in German).
[40] Cracow University of Technology. Tests covering measurements of noise, displacements and accelerations of vibrations of pavement and subgrade elements, stresses in rails on test sections on the CMK line during test runs of the Pendolino train with data analysis. Research Report, Cracow; 2014 (in Polish).
[41] Sheng X, Jones CJC, Thompson DJ. A theoretical model for ground vibration from trains generated by vertical track irregularities. J Sound Vib. 2004;272:937–65.
[42] Thompson D. Railway noise and vibration: mechanisms, modeling and means of control. Monograph, Institute of Sound and Vibration Research, University of Southampton. UK: Elsevier; 2009.
[43] Xia H, Cao YM, De Roeck G. Theoretical modeling and characteristic analysis of moving-train induced ground vibrations. J Sound Vib. 2010;329:819–32.
[44] Auersch L. The excitation of ground vibration by rail traffic: theory of vehicle-track interaction and measurements on high-speed lines. J Sound Vib. 2005;284:103–32.
[45] Taslagyan Karen A. The shear strength of granular soils under the influence of vibration. PhD thesis, University of Alberta. Canada: 2014.
[46] Ukleja J. C*onsideration of impact assessment of vibrations for strength and compression in silty soils*. MATEC Web of Conferences. 107, 2017. DYN-WIND'2017, pp. 1–6. p. 00030.
[47] PN-B-03020:1981: Construction soils–Direct foundations–Static calculations and design (standard superseded by Eurocode 7 PN-EN 1997–1:2008).